Accepted Manuscript

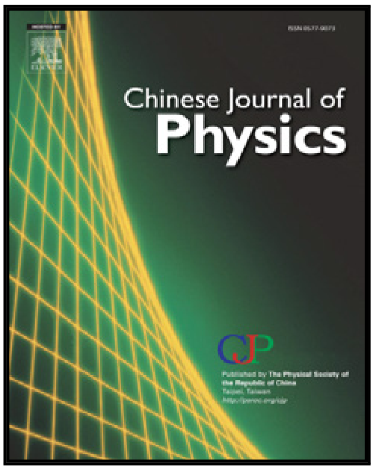

Heat transfer analysis for three-dimensional stagnation-point flow over an exponentially stretching surface

Fiaz Ur Rehman , S. Nadeem , R.U. Haq

PII: S0577-9073(17)30209-5
DOI: 10.1016/j.cjph.2017.05.006
Reference: CJPH 237

To appear in: *Chinese Journal of Physics*

Received date: 7 March 2017
Revised date: 9 May 2017
Accepted date: 9 May 2017

Please cite this article as: Fiaz Ur Rehman , S. Nadeem , R.U. Haq , Heat transfer analysis for three-dimensional stagnation-point flow over an exponentially stretching surface, *Chinese Journal of Physics* (2017), doi: 10.1016/j.cjph.2017.05.006

Highlights

- Flow over an exponentially stretching surface with heated wall is considered.
- Model is initiated for stagnation point that is not been explore in the literature so far.
- Homotopy analysis method (HAM) is used to tackle the nonlinear model.
- Dominant effects of heated wall within the boundary layer domain are presented.
- Local Nusselt number is plotted to determine the heat transfer rate at the surface.

Heat transfer analysis for three-dimensional stagnation-point flow over an exponentially stretching surface

Fiaz Ur Rehman[1], *S. Nadeem*[1], *R. U. Haq*[2*]

[1]*Department of Mathematics, Quaid-I-Azam University, Islamabad 44000, Pakistan*

[2]*Department of Electrical Engineering, Bahria University, Islamabad Campus, Islamabad, 44000, Pakistan*

Abstract:

In the current article, a detail investigation is accomplished to examine the laminar boundary-layer stagnation-point flow and heat transfer of a steady, three dimensional fluid caused by a surface which was stretched exponentially. After using the boundary layer approximation and suitable similarity transformation of exponential character, the resulting three dimensional non-linear momentum and energy equations are transmuted into nonlinear and non-homogeneous differential equations involving ordinary derivatives. Final equations are then solved out by applying homotopy analysis technique (HAM). The influence of dominating parameters on profiles of velocity and temperature are explained. The aspects of skin friction coefficient as well as Nusselt number are also computed. Graphical results of involved parameters are presented. It is found that results velocities and temperature profiles are strongly influenced by stretching ratios and stagnation point parameter. Friction at the surface is found to opposite trend along *x* and *y*-directions with respect the increasing values of stretching ratios parameters.

Keywords Heat transfer, exponential stretching, stagnation-point flow, three-dimensional flow, boundary layer.

1. Introduction

After the initial work done by Sakiadis [1,2] (1961) on flow determined by a continuously moving sheet, many researchers concentrated on Newtonian as well as non-Newtonian flow of fluids by applying boundary layer phenomena over linear and nonlinear stretching surfaces. The studies have been motivated by fundamental nature of boundary layer flows. Such flow and heat transport of viscous fluids in the region of boundary layer due to stretching surface has gained admirable attention as a result of its several useful uses in

* *Corresponding author: Rizwan Ul Haq (ideal_riz@hotmail.com)*

the process of manufacturing and in industries. Some of the applications include material manufactured by aerodynamic excursion and polymer excursion, glass fiber production, continuous plastic films stretching, metal excursion, artificial fibers, spinning of metal and petrochemical industries etc. As the world demand the highest quality of the manufacturing product in the stretching sheet process it is necessary to get precise control of flow and heat transfer. Therefore, Crane [3] (1970) examined work of Sakiadis analytically using a similarity transformation. Other researchers [4-9] extended the boundary –stretching problem to a variety of aspects, including the effects of suction or injection, power-law speed-driven surface, variable temperature surface, non-Newtonian or MHD fluids, porous media, thermal radiation, internal heat generation or absorption, mixed convection, and mass transport.

In above studies most of the work deals with a continuously moving surface with a constant or a linear stretching speed except results produced by Ali [5] (1995), who considered a power-law driven sheet problem. Unfortunately, not all speeds of the stretching sheet employed in industries are of a linear or a power-law type. Magyari and Keller [10] (1999) first considered steady 2-dimensional boundary layer flow when the settled sheet is stretched exponentially and they also analyzed the heat transport. Elbashbeshy [11] (2001) analyzed the suction effect on heat transfer aspects of the same exponentially stretching sheet problem. Khan and Sanjayanand [12, 13] investigated the flow, heat, and mass transport characteristic of the visco-elastic fluids for the flow described by Magyari (1999). Partha et al. [14] (2005) adopted a local similarity analysis to examine the influence of viscous dissipation due to mixed convection for viscous fluid over a sheet which was stretching exponentially. Abd El-Aziz [15] (2009) examined the mixed convection considered by Partha et al. (2005) in presence of the dissipation effect for micropolar fluid and Pal [16] (2010) investigated the effect of magnetic field for viscous fluid. More recently, Nadeem et al. [17] (2011) applied a series solution method to examine the thermal radiation effect on flow of viscous and Jeffrey fluids, respectively, because of an exponentially stretched surface. Bhattacharyya et al. [18] (2012) explored the heat transfer due to the stagnation-point flow when the sheet was shrunk exponentially. The boundary layer flow and heat and mass transport problem of nanofluids over an exponentially stretching surface was investigated by Nadeem and Lee [19] (2012) employing the homotopy analysis method. Liu and Wang [20] (2013) numerically examined, flow and heat transport of 3-D flow over a surface stretched exponentially. The results show that an accurate numerical solution can be obtained by applying a 5th order R-K scheme of integration along with a multidimensional method of tangents. Some of the recent studies reflect the major contribution of heat transfer phenomena near stagnation point flow of both Newtonian and non-Newtonian fluids [21-36].

To the best of our knowledge it is observed that flow and heat transport for 3-D stagnation-point flow over an exponentially stretching surface is not described in the avaliable literature by researchers. Thus based on the research above, this study analyzes the steady, three-dimensional heat transport characteristic of the stagnation point viscous fluid flow owing to a horizontal surface stretched exponentially. In this study, it is also presumed that the temperature specified at the stretching surface is distributed exponentially. Further, we employ a self-similar transformation to cut down the basic equations, under boundary-layer assumptions, to a collection of nonlinear ordinary differential equations. These equations are then tackled by using HAM. To make sure the convergence of desired solution, we plotted h-curve and constructed a convergence table. With the help of plotted graphs, we observed the impact of all parameters involved in this study. At last, tables are displayed to analyze the outcomes of significant parameters against skin friction coefficient and Nusselt number.

2. Mathematical model development

We now consider a steady, laminar and 3-D boundary layer stagnation-point flow and heat transfer over an exponentially stretching surface, having velocity components U_w and V_w in two directions of a Cartesian coordinate system (x, y, z) moving through a quiescent incompressible viscous fluid (see Figure 1). The surface is settled at $z = 0$ and flow is bound to $z \geq 0$. Moreover, T_w and T_∞ are constant temperature at wall and ambient fluid temperature respectively. After applying above suppositions the governing equation can be represented in usual notations as:

$$u_x + v_y + w_z = 0, \tag{1}$$

$$u(u_x) + v(u_y) + w(u_z) = \frac{1}{\rho}P_x + \nu(u_{zz}), \tag{2}$$

$$u(v_x) + v(v_y) + w(v_z) = \frac{1}{\rho}P_y + \nu(v_{zz}), \tag{3}$$

$$u(T_x) + v(T_y) + w(T_z) = \frac{k}{\rho c_p}(T_{zz}). \tag{4}$$

Associated boundary conditions are

$$\left.\begin{array}{c} u(z) = U_w(x,y), v(z) = V_w(x,y), w(z) = 0, T(z) = T_w(x,y) \text{ at } z = 0, \\ u(z) = U_s(x,y),\ v(z) = V_s(x,y),\ w(z) = 0,\ T(z) = T_\infty \text{ as } z \to \infty. \end{array}\right\} \quad (5)$$

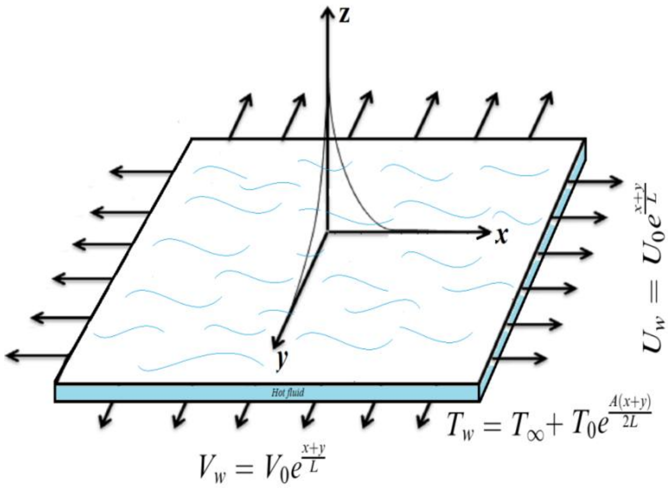

Figure 1: Geometry of the problem.

Where the velocity components are (u, v, w), T denotes the temperature, $\nu = \mu/\rho$ is the kinematic velocity, ρ represents mass per unit volume, k is known as thermal conductivity and c_p stands for specific heat when pressure is considered constant. The subscripts w and s are introduced to represent wall and free stream conditions respectively. In this study we assumed that the surface stretching velocities, wall temperature and free stream velocity are

$$U_w(x,y) = U_0 e^{\frac{x+y}{L}},\ V_w(x,y) = V_0 e^{\frac{x+y}{L}},\ T_w(x,y) = T_\infty + T_0 e^{\frac{A(x+y)}{2L}}. \quad (6)$$

$$U_s = U_e e^{\frac{x+y}{L}},\ V_s = V_e e^{\frac{x+y}{L}}. \quad (7)$$

Where T_0, U_0, V_0, U_e and V_e are all constants, T_∞ is ambient fluid temperature, L specifies reference length, and A intends the temperature exponent. We selected a similarity transformation by introducing new variables as [20]

$$\left.\begin{array}{c} u = U_e e^{\frac{x+y}{L}} f'(\eta), v = U_e e^{\frac{x+y}{L}} g'(\eta), \\ w = -\left(\frac{\nu U_e}{2L}\right)^{1/2} e^{\frac{(x+y)}{2L}} [f + \eta f' + g + \eta g'], \\ T = T_\infty + T_0 e^{\frac{A(x+y)}{2L}} \theta(\eta), \eta = \left(\frac{U_e}{2\nu L}\right)^{1/2} e^{\frac{(x+y)}{2L}} z. \end{array}\right\} \quad (8)$$

Where, A is temperature exponent. Now condition for incompressibility, Eq. (1) is satisfied identically and Equation (2)-(4) can be cast into a set of dimensionless ordinary differential equations (ODEs) expressed as

$$f''' = -f''(f+g) + 2f'(f'+g') - 2(1+r_1), \tag{9}$$

$$g''' = -g''(f+g) + 2g'(f'+g') - 2(1+r_1)r_1, \tag{10}$$

$$\theta'' = -\mathrm{Pr}\theta'(f+g) + \mathrm{Pr}A\,\theta(f'+g'), \tag{11}$$

The corresponding boundary conditions (5) will takes the following form

$$f(0) = 0 = g(0),\ f'(0) = \alpha_1,\ g'(0) = \alpha_2, \theta(0) = 1, \tag{12}$$

$$f'(\infty) = 1,\ g'(\infty) = r_1,\ \theta(\infty) = 0. \tag{13}$$

The primes in equations stand for differentiation with respect to η, $\alpha_1 = U_0/U_e$, $\alpha_2 = V_0/U_e$ are the stretching ratios, $r_1 = V_e/U_e$ is the stagnation point parameter and $Pr = \mu c_p/k$ is the Prandtl number. The first two equalities in Equation (12) originate from the no-penetration condition at the wall, $f(0) + g(0) = 0$. Without loss of generality, equation (12) is used instead. Note that the continuity equation (1) has been satisfied by assuming the form defined in Equation (8). Equations (9)-(13) demonstrate that the hydrodynamic non-homogeneous problem contains three parameters in the boundary conditions, while the heat transfer problem contains two additional parameters in the equation. The dimensionless skin-friction coefficient in both (x and y respectively) directions take the following form defined in equations (14)-(15)

$$c_{fx} = \frac{\tau_{wx}}{\rho U_e^2/2} = \frac{-\mu(\frac{\partial u}{\partial z} + \frac{\partial w}{\partial x})_{z=0}}{\rho U_e^2/2} = -\left(\frac{Re}{2}\right)^{-1/2} e^{\frac{3(x+y)}{2L}} f''(0), \tag{14}$$

and

$$c_{fy} = \frac{\tau_{wy}}{\rho U_e^2/2} = \frac{-\mu(\frac{\partial v}{\partial z} + \frac{\partial w}{\partial y})_{z=0}}{\rho U_e^2/2} = -\left(\frac{Re}{2}\right)^{-1/2} e^{\frac{3(x+y)}{2L}} g''(0), \tag{15}$$

Where Re symbolizes Reynolds number defined as $Re = U_e L/\nu$. We symbolized local Nusselt number by Nu_x and is given as

$$Nu_x = \frac{-k\frac{\partial T}{\partial z}|_{z=0}}{k\,(T - T_\infty)/x} = -\frac{x}{L}\left(\frac{Re}{2}\right)^{1/2} e^{\frac{x+y}{2L}}\,\theta'(0). \tag{16}$$

3. Solution technique

To obtain the solutions of Eqs (10)-(12), we adopted frequently used Homotopy analysis technique (HAM). It is a powerful analytic type technique for solving non-linear, ordinary as well as partial differential equations. In 1992, Liao [37] developed this analytical technique. This technique can be used to solve weak as well as strongly non-linear mathematical models due to the fact that it does not dependent on small physical parameter confinement. While using this technique we can adapt the convergence of solution using base functions and supplementary parameters. In the present study our initial guesses and their corresponding operators are listed below

$$\left.\begin{array}{c} f_0(\eta) = \eta + (\alpha_1 - 1)(1 - e^{-\eta}), \\ g_0(\eta) = (\alpha_2 - r_1) + r_1\eta + (r_1 - \alpha_2)(e^{-\eta}), \\ \theta_0(\eta) = e^{-\eta}. \end{array}\right\}. \tag{17}$$

Operators define for given set of differential equation are:

$$L_f(f) = \frac{d^3 f}{d\eta^3} - \frac{df}{d\eta},\ L_g(g) = \frac{d^3 g}{d\eta^3} - \frac{dg}{d\eta},\ L_\theta(\theta) = \frac{d^2\theta}{d\eta^2} - \theta. \tag{18}$$

4. Convergence analysis

The rapid convergence of solution obtained by Homotopy analysis technique greatly relies on the best selection of supplementary parameter h_f, h_g, h_θ. The usefulness of obtained solution highly depends on the rate of convergence. To make sure the convergence of resulting solution, combine h-curve is diagrammed at 20th order of approximation as represented in Fig. 2.

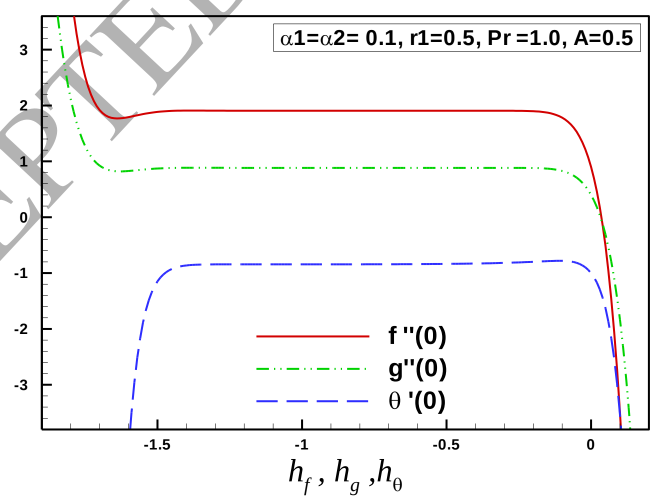

Figure 2: Combine plot for h curves.

Table 1: Convergence of Homotopy solution by taking a number of different estimations when $\boldsymbol{Pr = 0.5, \alpha1 = \alpha2 = 0.1, r1 = 0.5, A = 0.5, h_f = h_g = -0.8}$ and $\boldsymbol{h_\theta = -0.83.}$

Order of estimation	$f''(0)$	$g''(0)$	$-\theta'(0)$
1	1.647	0.770	0.567
6	1.903	0.882	0.714
12	1.906	0.883	0.724
18	1.906	0.884	0.728
24	1.906	0.884	0.730
30	1.906	0.884	0.730
40	1.906	0.884	0.730

In Fig. 2 we observe that the permissible range for h_f, h_g, h_θ is $-1.5 \leq h_f \leq -0.2$, $-1.5 \leq h_g \leq -0.2$, $-1.4 \leq h_\theta \leq -0.3$. After selecting suitable values for h_f, h_g and h_θ, we constructed a convergence table (Table 1) for $f''(0), g''(0), \theta'(0)$ by taking $h_f = h_g = -0.8$ and $h_\theta = -0.83$. After investigation of outcomes in above table, it is guaranteed that the desired convergence is attained at 24$^{\text{th}}$ order.

5. Final results and discussion

It is observed that in presence of stagnation point flow all velocities $f'(\eta)$ and $g'(\eta)$ begin from their wall values $\alpha1$ and $\alpha2$ respectively. As η increases, $f'(\eta)$ approaches 1 and $g'(\eta)$ approaches the stagnation point r1. The temperature profile $\theta'(\eta)$ decreases from unity (1) to zero (0) as dimensionless distance η grows from starting position zero to infinity. In Figure 3(a), we diagrammed the velocity component along x −direction and temperature transport profile for various inputs of stretching ratio $\alpha1$. As the stretching ratio $\alpha1$ increases, the velocity $f'(\eta)$ increases for $0 \leq \alpha1 \leq 1$ whereas $f'(\eta)$ decreases for $1 < \alpha1 \leq 2$. Also, it is concluded that as $\alpha1$ increases, the resulting temperature profile $\theta'(\eta)$ diminishes. Figure 2(b) shows the variation of velocity component along y −direction for stretching ratio $\alpha1$ where $0 < \alpha1 \leq 2$. The velocity and temperature graphs against different values of $\alpha2$ are aforethought in Fig. 4. It is clearly observed by looking at Fig. 4(a) that as $\alpha2$ increases, the velocity distribution $f'(\eta)$ and temperature profile $\theta'(\eta)$ show decreasing behavior. Figure 4(b) depicts the influence of stretching ratio $\alpha2$ on velocity component along y −direction. It is worth mentioning that the velocity gradient zero when $\alpha 2 = r1$, positive when $\alpha 2 < r1$ and negative when $\alpha 2 > r1$. In Figure 5(a), it is observed that as $r1$ increases, the velocities $f'(\eta)$ increases whereas temperature profile $\theta'(\eta)$ decreases. In Figure 5(b) we see that velocity profile along y −direction decreases when $r1 < 1$ and increases when $r1 > 1$. When $r1 = 1$, the identity $f = g$ is jumped, that is the axisymmetric stagnation-point flow of a stretching surface.

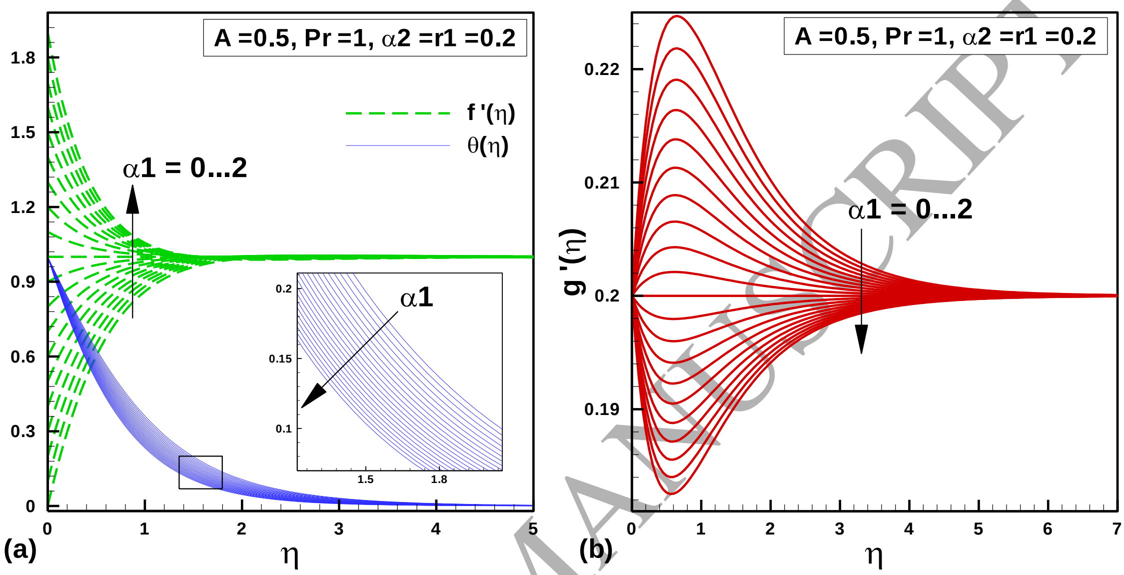

Figure 3(a)-3(b): Velocity & Temperature fluctuation against stretching ratio $\boldsymbol{\alpha 1}$.

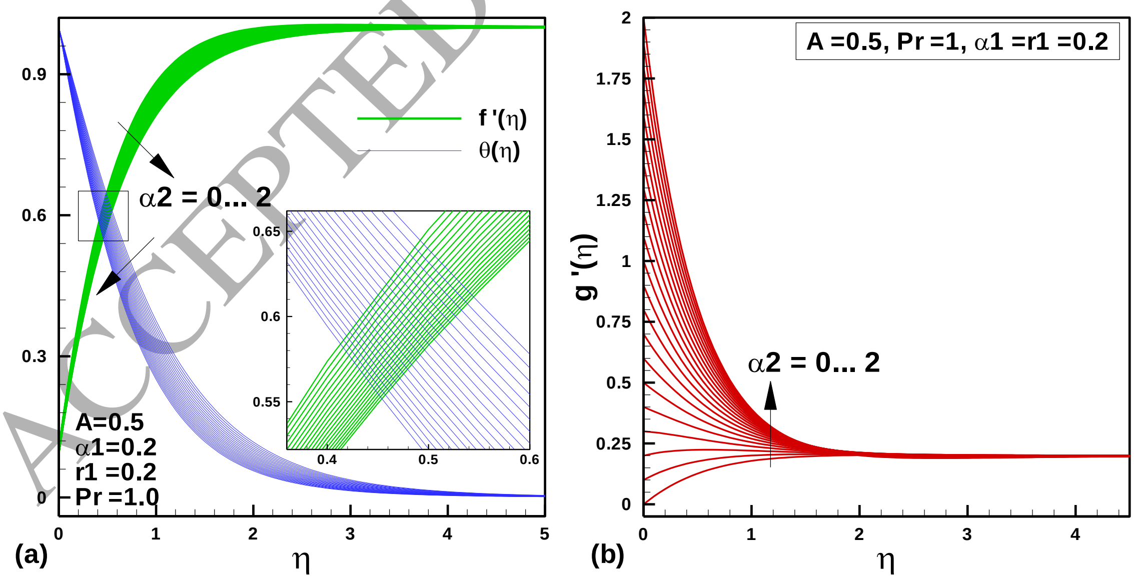

Figure 4(a)-4(b): Velocity & Temperature fluctuation against $\boldsymbol{\alpha 2}$.

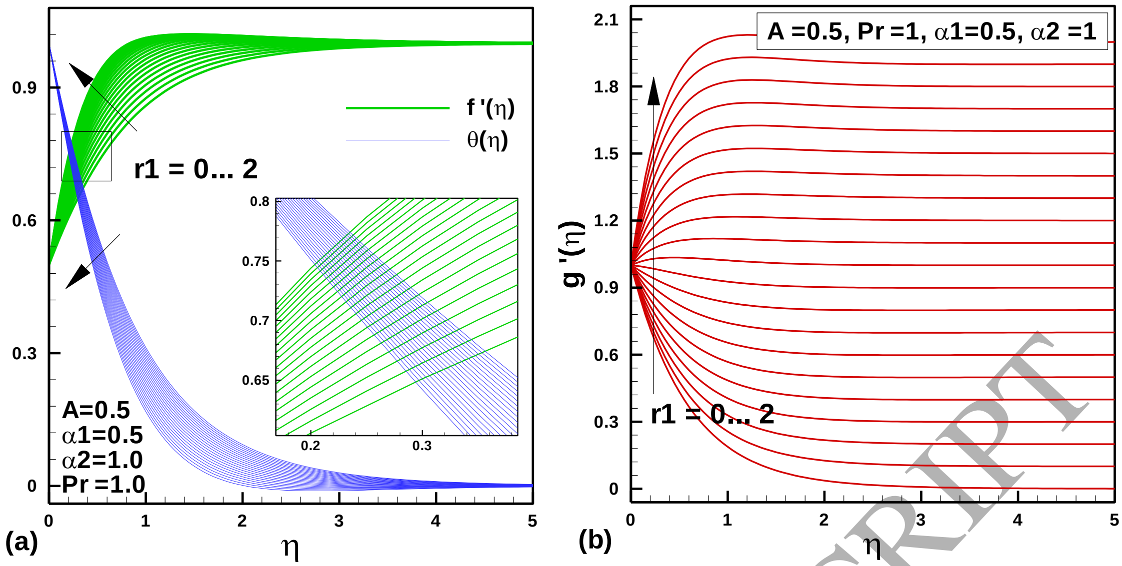

Figure 5(a)-5(b): Velocity & Temperature fluctuation against **$r1$**.

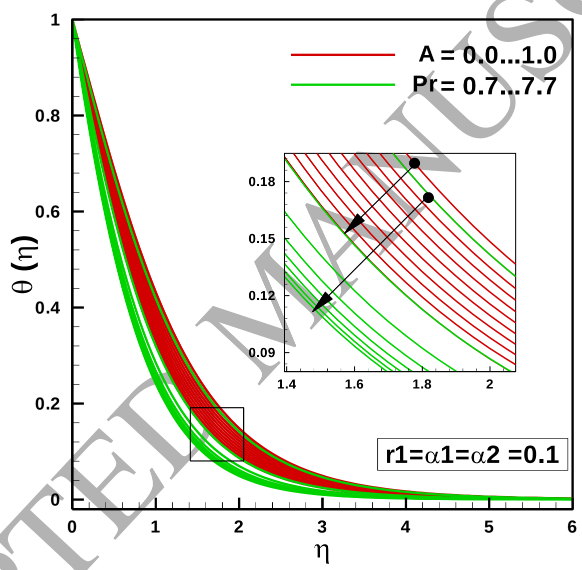

Figure 6: Temperature variation against **A** and **Pr**.

When we look at Figure 6, it depicts the impression of temperature exponent A and Prandtl number Pr on temperature profile $\theta(\eta)$ when $\alpha 1 = \alpha 2 = r1 = 0.1$. As temperature exponent A increases, the temperature profile $\theta(\eta)$ decreases. For A values, the temperature profiles show a decreasing behavior while depending on η. Correspondingly, thickness of occurring thermal boundary layer becomes thinner for enhancing A. Similarly, as Pr increases, temperature profile $\theta(\eta)$ decreases and as an outcome our thickness of thermal boundary layer becomes thinner for increasing Pr which owes to the smaller thermal diffusive effects.

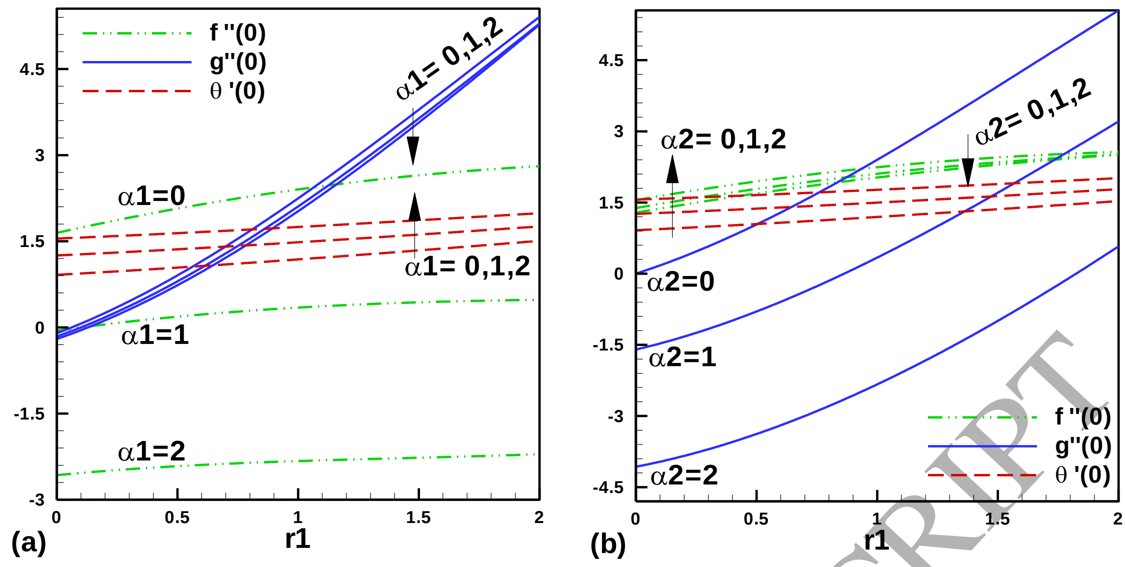

Figure 7(a)-7(b): Influence of $\boldsymbol{\alpha 1}$ and $\boldsymbol{\alpha 2}$ Vs. $\boldsymbol{r1}$ on Skin-friction $\boldsymbol{C_f}$ and Nusselt number $\boldsymbol{Nu_x}$.

The variation in the skin frictions as well as the heat transport rate under influence of active parameters are demonstrated in Figures 7(a), 7(b), 8(a) and 8(b) one by one. Figure 7(a) and 7(b) show change in $\theta'(0)$, $f''(0)$ and $g''(0)$ vs. $r1$ for diverse values of $\alpha 1$ and $\alpha 2$ respectively. We can easily depicted that $f''(0)$ and $g''(0)$ decrease whereas $\theta'(0)$ increases for increasing values of $\alpha 1$ and $\alpha 2$ respectively. The variation of $\theta'(0)$ vs. Prandtl number Pr for several quantities of $\alpha 1$, $\alpha 2$ and $r1$ are sketched in the Figure 8(a) and 8(b) taking $A = -1,\ 0,\ 1$. By taking $A = 0,\ 1,$ the heat transport rate increases when Pr enhances for increasing numbers of $\alpha 1$, $\alpha 2$ and $r1$. On the other hand the dimensionless heat transport rate decreases for increasing inputs of Pr when $A = -1$.

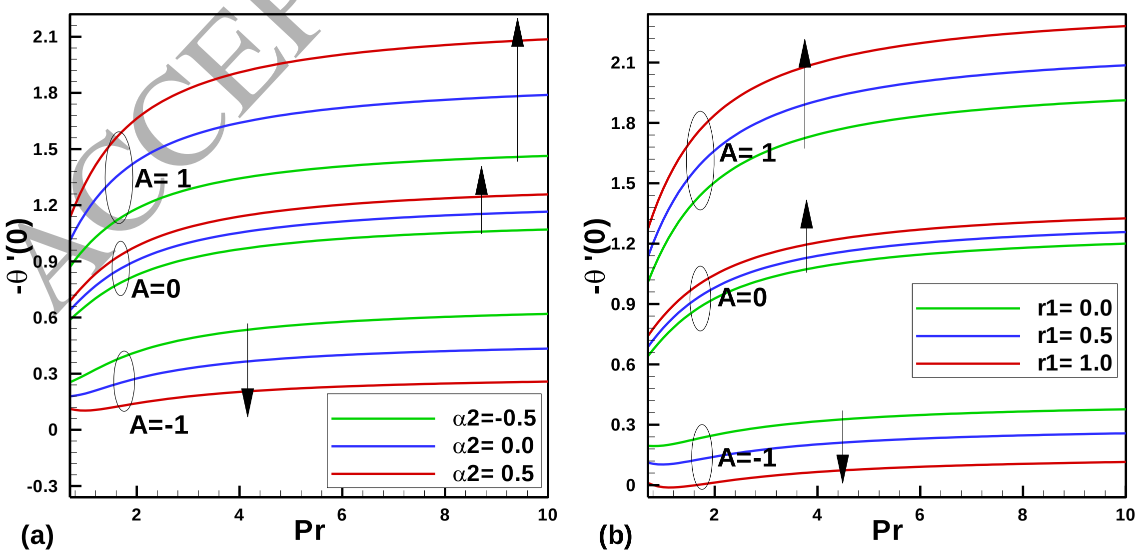

Figure 8(a)-8(b): Fluctuation in Nusselt number along temperature exponent $\boldsymbol{A}$ for $\boldsymbol{\alpha 2}$ and $\boldsymbol{r1}$ with various values of **Pr**.

Table 2: Numerical results of the present study for Nusselt Number $\boldsymbol{\theta'(0)}$ taking $\boldsymbol{h_\theta = -0.83, \alpha_1 = 0.1, \alpha_2 = 0.1, r_1 = 0.5}$.

Pr	A	$-\boldsymbol{\theta'(0)}$
1	-1.5	0.246385
	0	0.703287
	1.5	1.113360
	3	1.476620
5	-1.5	0.490342
	0	1.009240
	1.5	1.481320
	3	1.906580
10	-1.5	0.534615
	0	1.061270
	1.5	1.541100
	3	1.974100

Table 2 demonstrates different inputs for Nusselt number for increasing Prandtl number symbolized as Pr and A, denoting temperature exponent. The heat transfer rate $|\theta'(0)|$ increase with increasing temperature exponent A. Similarly, the heat transfer rate $|\theta'(0)|$ increases when Pr is increased. It happens because of the conception that caloric boundary layer thickness present in viscous fluid diminishes with increasing values of Pr, as shown in Fig 4. Numerical outcomes related to Skin-friction are represented in Table 3 taking $h_f = h_g = -0.8$.

Table 3: Numerical results of the present study for Skin-friction coefficients taking $\boldsymbol{h_f = h_g = -0.8}$.

$\boldsymbol{\alpha 1}$	$\boldsymbol{\alpha 2}$	$\boldsymbol{r1}$	$\boldsymbol{f''(0)}$	$\boldsymbol{g''(0)}$
0	**0**	**0**	1.59459	0
		0.5	2.02849	1.01424
		1	2.42309	2.42309
	0.5	**0**	1.53668	-0.609375
		0.5	1.96418	0.284
		1	2.35238	1.5513
	1	**0**	1.48988	-1.48988

		0.5	1.91098	-0.6946
		1	2.29278	0.453926
0.5	**0**	**0**	0.927301	0
		0.5	1.26609	0.982089
		1	1.5513	2.35238
	0.5	**0**	0.744938	-0.744938
		0.5	1.08593	0.130444
		1	1.37335	1.37335
	1	**0**	0.591242	-1.72589
		0.5	0.934444	-0.934444
		1	1.22407	0.203852
1	**0**	**0**	0	0
		0.5	0.260889	0.955489
		1	0.453926	2.29278
	0.5	**0**	-0.271704	-0.862946
		0.5	0	0
		1	0.203852	1.22407
	1	**0**	-0.497185	-1.9268
		0.5	-0.214667	-1.13362
		1	0	0

6. Conclusions

This investigation is concerned with flow and heat transport for 3-D stagnation-point flow caused by a surface stretched exponentially. This study also assumes that the temperature specified at the surface varies exponentially. The developed mathematical model is tackled by homotopy analysis technique. We observed in current study that an increase in wall stretching ratio $\alpha 1$ along $x-$axis increases $f'(\eta)$ whereas decreases $g'(\eta)$ and temperature field. Following are the major finding of whole analysis

- An increase in wall stretching ratio $\alpha 2$ along $y-$axis increases $g'(\eta)$ whereas decreases $f'(\eta)$ and temperature field.
- The increasing stagnation-point parameter $r1$ increases dimensionless velocity distribution in both directions and decrements the temperature distribution.
- Increasing Temperature exponent A and Prandtl number Pr decrease dimensionless temperature profile.
- Table 2 shows that heat flux increases by increasing temperature exponent or Prandtl number.
- Table 3 shows numerical outcomes for skin-friction which is observed in both $x-$ and $y-$ directions.

7. References

[1] B. C. Sakiadis, Boundary- layer behavior on continuous solid surface I. Boundary layer equations for two dimensional and axisymmetric flow, Journal American Institute of Chemical Engineers, 7 (1961) 26-28.

[2] B. C. Sakiadis, Boundary layer behavior on continuous solid surface. II. Boundary layer on a continuous flat surface, Journal American Institute of Chemical Engineers, 7 (1961) 221-225.

[3] L. Crane, Flow past a stretching plate, Zeitschrift fur Angewandte Mathematik and Physik., 21 (1970) 645-647.

[4] L. J. Grubka, and K. M. Bobba, Heat transfer characteristics of a continuous stretching surface with variable temperature, Journal of Heat and Transfer, 107 (1985) 248-250.

[5] M. E. Ali, On thermal boundary layer on a power-law stretched surface with suction and injection, Int. J. Heat Fluid Flow., 16 (1995) 280-290.

[6] H. I. Andersson, MHD flow of a viscoelastic fluid past a stretching surface, Acta Mech., 95 (1992) 227-230.

[7] K. V. Prasad, S. Abel, and P. S. Datti, Diffusion of chemically reactive species of a non-newtonian fluid immersed in a porous medium over a stretching sheet, Int. J. Non-linear Mech., 38 (2003) 651-657.

[8] I-C. Liu, Flow and heat transfer of an electrically conducting fluid of second grade in porous medium over a stretching sheet subject to a transverse magnetic field, Int. J. Non-linear Mech., 40 (2005) 465-474.

[9] C. H. Chen, On the analytic solution of MHD flow and heat transfer for two types of viscoelastic fluid over a stretching sheet with energy dissipation, internal heat source and thermal radiation, Int. J. Heat Mass Transfer., 53 (2010) 4264-4273.

[10] E. Magyari, and B. Keller, Heat and mass transfer in the boundary layer on an exponentially stretching continuous surface, J. Phys. D: Appl. Phys., 32 (1999) 577-585.

[11] E. M. A. Elbashbeshy, Heat transfer over an exponentially stretching continuous surface with suction, Arch. Mech., 53 (2001) 643-651.

[12] S. K. Khan, and E. Sanjayanand, Viscoelastic boundary layer flow and heat transfer over an exponentially stretching sheet, Int. J. Heat Mass Transfer., 48 (2005) 1534-1542.

[13] S. K. Khan, Boundary layer viscoelastic fluid flow over an exponentially stretching sheet, Int. J. Appl. Mech. Eng., 11 (2006) 321-335.

[14] M. K. Partha, P. V. S. N. Murthy, and G. P. Rajasekhar, Effect of viscous dissipation on the mixed convection heat transfer from an exponentially stretching surface, Heat Mass Transfer, 41 (2005) 360-366.

[15] M. Abd El-Aziz, Viscous dissipation effect on mixed convection flow of a micropolar fluid over an exponentially stretching sheet, Can. J. Phys., 87 (2009) 359-368.

[16] D. Pal, Mixed convection heat transfer in the boundary layer on an exponentially stretching surface with magnetic field, Appl. Math. Comput., 217 (2010) 2356-2369.

[17] S.Nadeem, S. Zaheer, and T. Fang, Effects of thermal radiation on the boundary layer flow of a Jeffrey fluid over an exponentially stretching surface, Numer. Algorithms., 57 (2011) 187-205.

[18] K. Bhattacharyya, K. Vajravelu, Stagnation-point flow and heat transfer over ab exponentially shrinking sheet, Commun. Nonlinear. Sci. Numer. Simulat., 17 (2012) 2728-2734.

[19] S. Nadeem, and C. H. Lee, Boundary layer flow of nanofluid over an exponentially stretching surface, Nanoscale Res. Lett., 7(1) (2012) article 94.

[20] C. Liu, Hung-H. Wang, Yih-F. Peng, Flow and heat transfer for three-dimensional flow over an exponentially stretching surface. Chemical Engineering Communications, 200 (2013) 253-268.

[21] S. Munawar, A. Mehmood, A. Ali, Time-dependent flow and heat transfer over a stretching cylinder, Chinese J. Phys., 50 (2012) 828-848.

[22] H. A. Attia, A. L. Aboul-Hassan, M. A. M. Abdeen, A. El-Din Abdin, W. Abd El-Meged, Unsteady couette flow of a thermally conducting viscoelastic fluid under constant pressure gradient in a porous medium, Chinese J. Phys., 52 (2014) 1015-1027.

[23] A. Shahzad, R. Ali, Approximate analytic solution for magneto-hydrodynamic flow of a non-newtonian fluid over a vertical stretching sheet. Canadian Journal of Applied Sciences, 2 (2012) 202-215.

[24] M. Khan, R. Ali, A. Shahzad, MHD Falkner-Skan flow with mixed convection and convective boundary conditions, Walailak Journal of Science and Technology (WJST), 10 (5) (2013) 517-529.

[25] A. Shahzad, R. Ali, MHD flow of a non-newtonian power law fluid over a vertical stretching sheet with the convective boundary condition, Walailak Journal of Science and Technology (WJST), 10 (1) (2013) 43-56.

[26] J. Ahmed, T. Mahmood, Z. Iqbal, A. Shahzad, R. Ali, Axisymmetric flow and heat transfer over an unsteady stretching sheet in power law fluid, Journal of Molecular Liquids, 221 (2016) 386–393.

[27] J. Ahmed, A. Shahzad, R. Ali, Convective heat transfer of a viscous fluid over a stretching sheet embedded in a thermally stratitified medium, accepted in: Bulgarian chemical communication, 2016.

[28] S. Nadeem, R.U. Haq, Z.H. Khan, Numerical solution of non-newtonian nanofluid flow over a stretching sheet, Appl Nanosci., 4(5) (2014) 625-631.

[29] S. Nadeem, R.U. Haq, Z.H. Khan, Heat transfer analysis of water-based nanofluid over an exponentially stretching sheet, Alexandria Engineering Journal, 53(1) (2014) 219-224.

[30] S. Nadeem, R.U. Haq, C. Lee, MHD flow of a casson fluid over an exponentially shrinking sheet, Scientia Iranica, 19 (2012) 1550-1553.

[31] M. Khan, Hashim, Boundary layer flow and heat transfer to carreau fluid over a nonlinear stretching sheet, AIP Advances, 5 (2015) 107203.

[32] M. Khan, Hashim, Ali Saleh Alshomrani, MHD stagnation-point flow of a carreau fluid and heat transfer in the presence of convective boundary conditions, PLOS ONE 11(6) (2016) 0157180.

[33] M. Khan, Hashim, Ali Saleh Alshomrani, Characteristics of melting heat transfer during flow of carreau fluid induced by a stretching cylinder, Eur. Phys. J. E, (2017) 40:8.

[34] Hashim, M. Khan, On cattaneo–christov heat flux model for carreau fluid flow over a slendering sheet, Results in Physics, 7 (2017) 310-319.

[35] Y. Shagaiya Daniel, Z. A. Aziz, Z. Ismail, F. Salah, Effects of thermal radiation, viscous and Joule heating on electrical MHD nanofluid with double stratification, Chinese Journal of Physics, 55(3) (2017) 630-651.

[36] S. Saleem, M. Awais, S. Nadeem, N. Sandeep, T. Mustafa, Theoretical analysis of upper-convected Maxwell fluid flow with Cattaneo-Christov heat flux model, Chinese Journal of Physics, (2017). doi.org/10.1016/j.cjph.2017.04.005.

[37] S. J. Liao, Beyond perturbation: introduction to the homotopy analysis method. CRC press LLC, 2004.

Graphical Abstract:

Analysis is performed for stagnation point flow over a stretching sheet. These important results are describing the behavior of unknown profiles of velocity and heat transfer.